Accepted Manuscript

Flame retardant efficiency of KH-550 modified urea-formaldehyde resin cooperating with ammonium polyphosphate on polypropylene

Ying Ren, Dandan Yuan, Wenmin Li, Xufu Cai

PII: S0141-3910(18)30092-2

DOI: 10.1016/j.polymdegradstab.2018.03.014

Reference: PDST 8488

To appear in: *Polymer Degradation and Stability*

Received Date: 9 November 2017

Revised Date: 11 March 2018

Accepted Date: 17 March 2018

Please cite this article as: Ren Y, Yuan D, Li W, Cai X, Flame retardant efficiency of KH-550 modified urea-formaldehyde resin cooperating with ammonium polyphosphate on polypropylene, *Polymer Degradation and Stability* (2018), doi: 10.1016/j.polymdegradstab.2018.03.014.

Flame retardant efficiency of KH-550 modified urea-formaldehyde resin cooperating with ammonium polyphosphate on polypropylene

Ying Ren, Dandan Yuan, Wenmin Li, Xufu Cai[1]

Department of Polymer Science and Materials, The State Key Laboratory of Polymer Materials Engineering, Sichuan University, Chengdu 610065, China

Abstract：

This paper surveys the char forming effect of urea-formaldehyde resin (UF) and the flame retardancy of UF cooperating with ammonium polyphosphate (APP) for polypropylene (PP). UF was firstly synthesized and then modified by a silane coupling agent 3-aminopropyltriethoxysilane (KH-550). UF and KH-550 modified urea-formaldehyde resin (M-UF) were characterized by field-emission scanning electron microscope (FE-SEM), energy-dispersive analysis (EDS), Fourier transform infrared spectroscopy (FTIR) and thermogravimetric analysis (TGA). Compared with UF, M-UF had better thermal stability and higher mass of residue char. Afterwards the intumescent flame retardants (IFRs), consisting of UF+APP and M-UF+APP respectively, were introduced into PP. The flame retardant efficiency of PP composites was investigated by limiting oxygen index (LOI), UL-94 vertical burning, and micro combustion calorimetry (MCC). The possible decomposition mechanisms were investigated by TGA, FT-IR and EDS. When the addition of PP, APP and UF was 70, 24 and 6wt%, the LOI value reached 23.5 and UL-94 test could not pass. However, when the loading of PP, APP and M-UF was 70, 20 and 10wt%, the LOI value reached 29.5 and UL-94 test was V-0. The residual char layers of some PP composites were analyzed by Laser Raman spectroscopy (LRS) and FE-SEM. The LRS and FE-SEM presented that the char layer of 20%APP+10%M-UF/PP was more compact

[1] Corresponding author.
E-mail address: caixf2008@scu.edu.cn (Xufu Cai)

and had higher strength than 20%APP+10%UF/PP. Furthermore, tensile tests showed that M-UF/APP could improve break strength and toughness for PP compared with the same ratio of UF/APP. To sum up, M-UF+APP/PP have better flame retardant efficiency and tensile properties compared with UF+APP/PP.

Keywords: urea-formaldehyde; KH-550 modified urea-formaldehyde; ammonium polyphosphate; intumescent flame retardants; polypropylene.

1. Introduction

Polypropylene (PP) is widely applied in the field of automobiles, electronics, and buildings and so on for its excellent characteristics such as mechanical properties, electric insulation and lightweight. However, inflammability and a mass of molten dripping limit PP applications and development. It is essential that flame retardant efficiency of PP should be improved [1, 2].

Intumescent flame retardants (IFRs) systems generally are comprised of dehydrating agent, charring agent and foaming agent, which are regarded as eco-friendly flame retardant because they generate less smoke and toxic substances during combustion. Traditional IFRs system contains ammonium polyphosphate (APP) as dehydrating agent, pentaerythritol (PER) as charring agent and melamine as foaming agent. IFRs are thought of a new generation flame retardants for polyolefin, particularly for PP that is significant but combustible commodity plastic [3-5]. IFRs systems nowadays have been developed rapidly, especially dehydrating agent and foaming agent tending to be mature. However, the disadvantages of traditional polyhydroxy charring agent, such as moisture absorption and poor compatibility with matrix, reduce mechanical properties of the related composites. Therefore it is significant to study out new applicable charring agent [6]. Urea-formaldehyde resin (UF) is namely synthesized through urea and formaldehyde. It is widely used as adhesive in woodworking industry for its inexpensiveness, insulation and resistance of weak acid or alkali [7-9]. Besides, UF is a hydroxyl polymer with high contents of carbon and nitrogen that benefit the flame retardant effect.

The purpose of this work firstly is to study the effect of char forming of UF. Moreover, in order to further improve its charring and flame retardancy, a silane coupling agent 3-aminopropyltriethoxysilane (KH-550) is used to modify UF. Therefore, KH-550 modified urea-formaldehyde resin (M-UF) includes flame-retardant elements both nitrogen and silicon. Silicon-containing compounds could form a protective silicon layer during inflaming, which could protect polymers from further thermal decomposition. Hence the flame retardancy of M-UF may be markedly improved for the synergistic effects of nitrogen and silicon [10, 11]. Then the IFRs, UF and M-UF respectively cooperating with ammonium polyphosphate (APP), are introduced into PP. The flame retardant efficiency of PP composites are mainly studied, and their tensile properties are studied briefly as well [12].

2. Experimental

2.1 Materials

Urea, formaldehyde solution (37-40wt%), KH-550 and distilled water all were purchased from Chengdu KeLong Chemical Industry Company. APP (degree of polymerization >1500) was a commercial product of Zhejiang Long you GD Chemical Industry Company. PP (S1003) was purchased from Duzishan petrochemical branch of Petro China. All chemicals were analytical reagents and used without further purification in this work. The structures of KH-550 and APP are shown in Scheme 1 and Scheme 2 respectively.

2.2 Samples preparation

To obtain M-UF, three step reactions were performed as shown in Scheme 1, where the synthetic procedures and the structures of UF and M-UF were explained as well.

2.2.1 Synthesis of urea-formaldehyde (UF) resin.

90g of urea, 112.5mL of formaldehyde solution and 45mL of distilled water were added into a 500mL three-necked and round-bottom glass flask which was equipped with a mechanical stirrer, a thermometer and a condenser. The PH value of reaction

mixture kept in 5-6 during whole reaction process. The temperature was firstly raised to 40□ and maintained for 40min, then heated to 60□ and maintained for 140min. After cooling to room temperature, 100g of suspension was taken out to further modify, and the rest was filtered and washed with distilled water [13-15]. The white powder, UF, was dried at 140□ for 24h.

2.2.2 Synthesis of KH-550 modified urea-formaldehyde (M-UF) resin.

Firstly, 100g of KH-550 was slowly added into 25mL of distilled water under stirring for 20min. Then the hydrolysate of KH-550 was slowly injected into 100g of UF under mechanical stirring. The reactive system was kept at 60□ for 1.5h [16-18]. Finally, the reaction product was filtered and washed with ethanol and distilled water. The pale yellow powder, M-UF, was also dried at 140□ for 24h.

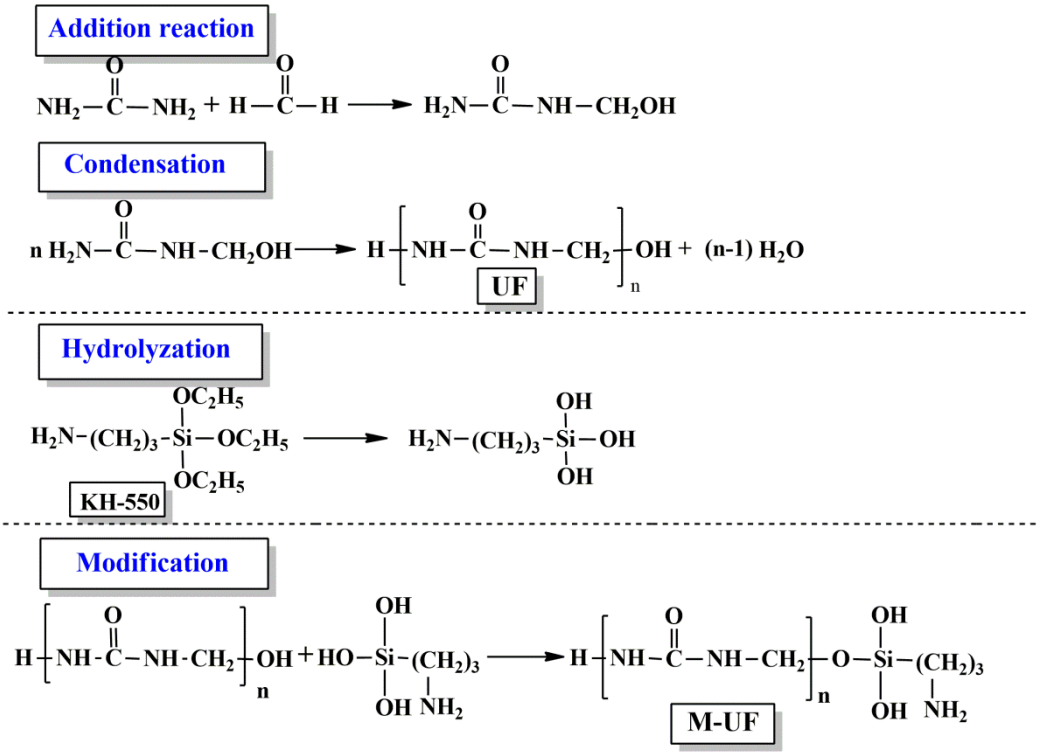

Scheme 1 The synthetic reactions of UF and M-UF.

2.2.3 Preparation of PP composites.

Two kinds of IFRs were composed of UF+APP and M-UF+APP respectively. PP was blended with the IFRs via a HAAKE plastic order mixer at 170□ and 60rpm for 10min. The PP composites afterwards were molded using a testing hot-press at 180□

to obtain different standard testing bars by plate vulcanizer (Qingdao Huabo Machinery Technology Co. Ltd. China). The compositions of PP composites are illustrated in Table 1.

Table 1 The compositions and flame properties of PP composites.

Samples	Components (wt%)				LOI (%)	UL-94
	PP	APP	UF	M-UF		
PP-1	**100**	**0**	**0**	**0**	**17**	**burning, dripping**
PP-2	**70**	**30**	**0**	**0**	**19.4**	**burning, dripping**
PP-3	**70**	**25**	**5**	**0**	**21.7**	**burning, dripping**
PP-4	**70**	**24**	**6**	**0**	**23.5**	**burning, dripping**
PP-5	**70**	**22.5**	**7.5**	**0**	**22.2**	**burning, dripping**
PP-6	**70**	**20**	**10**	**0**	**22**	**burning, dripping**
PP-7	**70**	**15**	**15**	**0**	**22**	**burning, dripping**
PP-8	**70**	**25**	**0**	**5**	**28**	**V-0**
PP-9	**70**	**24**	**0**	**6**	**27.5**	**V-0**
PP-10	**70**	**22.5**	**0**	**7.5**	**28**	**V-0**
PP-11	**70**	**20**	**0**	**10**	**29.5**	**V-0**
PP-12	**70**	**15**	**0**	**15**	**28.5**	**V-0**

2.3 Characterization and testing

Field-emission scanning electron microscope (FE-SEM) and energy-dispersive analysis (EDS). The surface morphologies and element analysis of samples were observed by FE-SEM (Nova NanoSEM450, FEI) and EDS (QUANTA 250, FEI) respectively.

Fourier transform infrared spectroscopy (FTIR). FTIR was recorded by a Nicolet IS50 spectrophotometer using KBr pellets, and the wavenumbers ranged from 4000 to 400cm^{-1}.

Thermogravimetric analysis (TGA). The thermostability of samples was measured by a TG-209 F1 thermal analyzer (Germany, Netzsch) in 5-8mg, nitrogen atmosphere, testing temperature ranging from 30 to 800□, and with heating rate of 10□/min.

Limiting oxygen index (LOI). LOI tests were performed by HC-2 oxygen index instrument produced by Jiangning Analysis Instrument Factory; with a specimen dimension of 130×6.5×3mm^3 according to ASTM D2863-08.

UL-94 vertical burning testing. The tests were carried out with a CFZ-2 measurement purchased from Jiangning Analysis Instrument Factory. The dimensions of each specimen were 125×12.5×3.2mm^3 according to the American National Standard UL-94 (ANSI/ASTM D635-77).

Micro combustion calorimetry (MCC). The combustion characteristic parameters of samples in 3-4mg were characterized by a FAA MCC (Fire Testing Technology, UK) according to ASTM D7309-07. The samples were heated from 100 to 700□ approximately at 1□/s and the combustor temperature was set at 900°C. The mixed nitrogen/oxygen flow rate was set as 80/20mL/min.

Muffle furnace. The residual char at different temperatures was obtained using Muffle furnace (Henan SanTe Furnace Technology Co., Ltd).

Laser Raman spectroscopy (LRS). The degree of graphitization for residual char was characterized by DXR 532 nm LASER. The char was obtained after LOI tests.

Tensile tests. Tensile tests of some PP composites were carried out through Universal Material Testing Machine produced by INSTRON with an extensional rate of 20±2 mm/min at room temperature, according to ASTM D882. The dimension of these samples was 4×75 dumbbell-shaped. Every testing specimen was measured 5 times and calculated to obtain average.

3. Results and discussion

3.1 Characterization of UF and M-UF

Fig.1 shows three kinds of magnification of the FE-SEM and EDS to observe the surface morphologies and analyze elements of UF and M-UF respectively. Table 2 presents the elements and their contents of UF and M-UF. There was no big difference in dispersibility of UF and M-UF. The surface of UF was shaggy and multi-hole, but M-UF was rough and compact. The EDS illustrated that UF mainly had high contents of C and N, but beyond those, M-UF had Si.

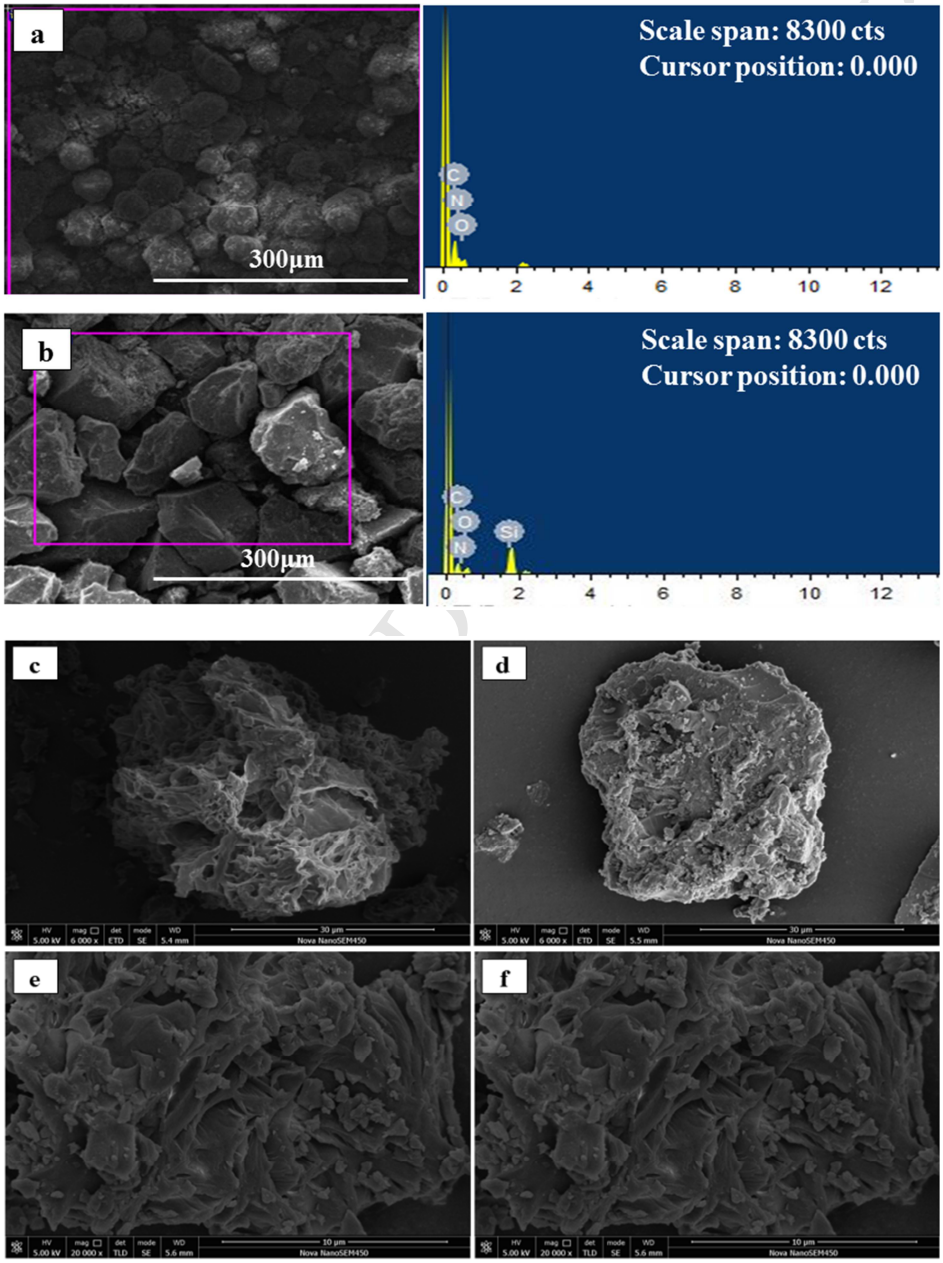

Fig.1 The FE-SEM images and EDS analysis of UF (a, c, e) and M-UF (b, d, f).

Table 2 The elements and their contents of UF and M-UF obtained from EDS.

Elements	C (wt%)	N (wt%)	O (wt%)	Si (wt%)
UF	**32.3**	**38.5**	**29.2**	**0**
M-UF	**38.3**	**21.9**	**28.1**	**11.7**

Fig.2 presents the FTIR spectra of UF, M-UF and KH-550. The broad and strong absorption peak at 3200−3600cm^{-1} that belonged to the stretching vibration of -OH appeared in both UF and M-UF [19]. It meant that the chemical environment of -OH was complicated and diverse. Besides, the stretching vibrations of –NH_2 and -NH were not obvious. The absorption peak of C-O in UF terminal C-OH at 1004cm^{-1} was disappeared in M-UF, which illustrated that the hydroxyl or amine of KH-550 had a reaction with terminal hydroxyl of UF. In M-UF, the new absorption peak of Si-O in Si-OH at 921cm^{-1} appeared, but the peak of dissociative Si-OH at 3690cm^{-1} did not appear. Additionally, the new absorption peaks at 1194 and 467cm^{-1} were antisymmetric stretching vibration and flexural vibration of Si-O-Si. From the results, it seemed that dehydration-condensation was happened in some Si-OH, and the rest Si-OH might form intermolecular hydrogen bonds. Therefore, the peak of -OH shifted towards lower wavenumbers (3200-3400cm^{-1}).

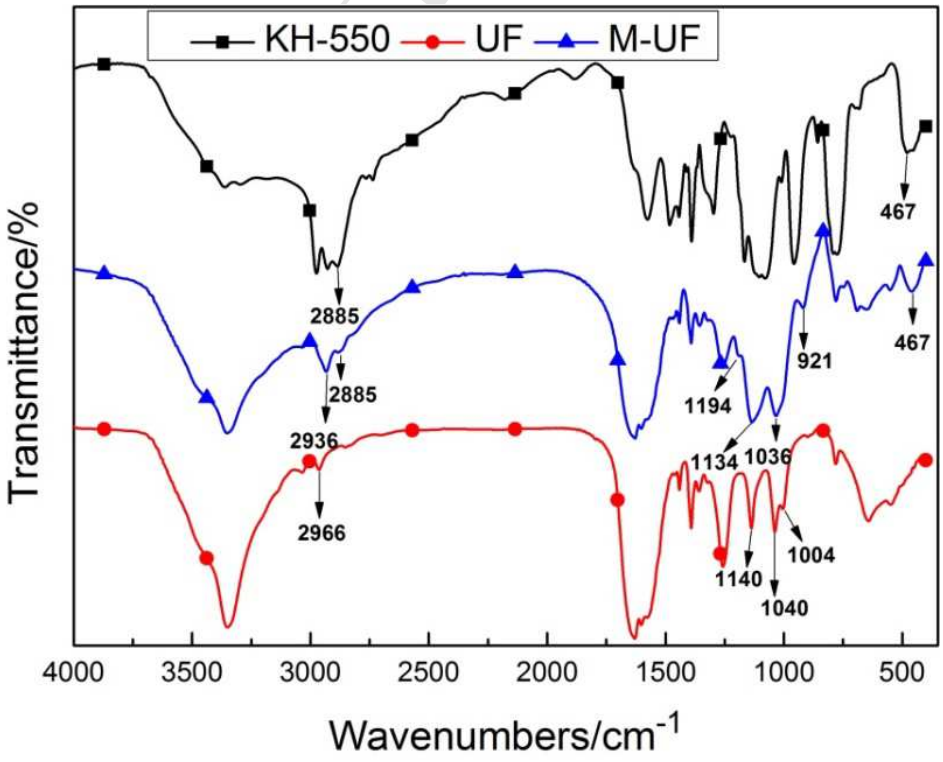

Fig.2 The FTIR spectra of UF, M-UF and KH-550.

The peak at 2966cm^{-1} was attributed to antisymmetric stretching vibration of -CH_2- in UF, but the relative peak occurred at 2936cm^{-1} in M-UF because -CH_2-OH was changed into -CH_2-O-Si. The electronegativity of the groups connected with -CH_2- was weakened, which led to the reduction of force constant and characteristic frequency. The new peak at 2885cm^{-1} in M-UF belonged to the stretching vibration of -CH_2- in Si-CH_2-CH_2-CH_2-, which was corresponded with KH-550. In UF, the peaks at 1040 and 1140cm^{-1} were attributed to the stretching vibration of C-O-C, which suggested that among hydroxyls of hydroxymethyl urea formed ether linkage by dehydration synthesis. However, the wavenumbers of ether linkage moved to 1036 and 1134cm^{-1} in M-UF, because C-O-C was replaced by C-O-Si through the dehydration condensation between the Si-OH in hydrolytic KH-550 and the C-OH in UF [16, 20, 21]. The electronegativity of silicon was lower than carbon, so the characteristic frequencies of ether linkage were reduced. All above-mentioned indicated that KH-550 had successfully modified UF and introduced silicon into UF.

In order to further research the modification of KH-550 to UF, the thermal decompositions of UF, KH-550, M-UF and UF+KH-550 cal. are presented by Fig.3a thermogravimetric (TG) behaviors and Fig.3b derivative thermogravimetric (DTG) behaviors.

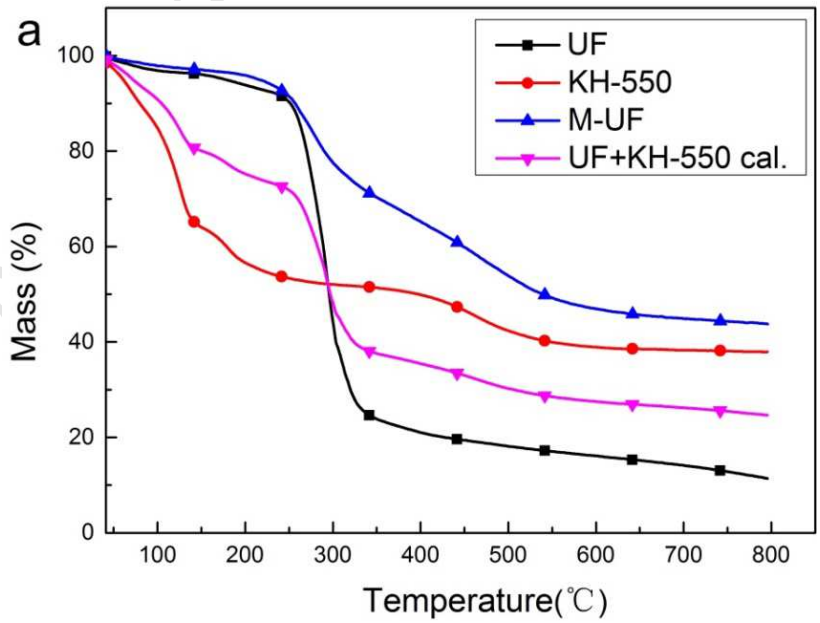

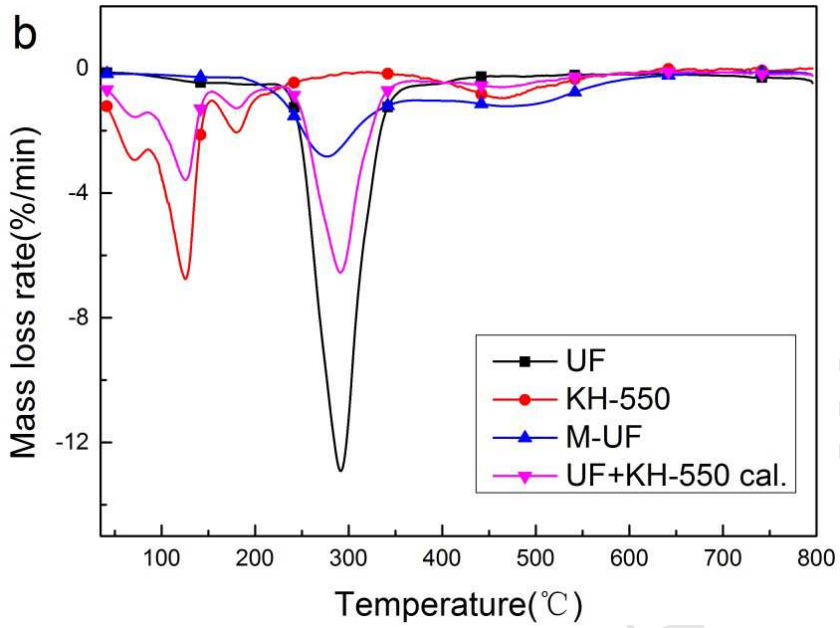

Fig.3 The TG (a) and DTG (b) curves of UF and M-UF.

UF+KH-550 cal.: the average of UF and KH-550.

As shown in the Fig.3a, UF had one step decomposition and the temperature of 5% mass loss ($T_{5\%}$, the same below) was 177□, which was attributed to the evaluation of H_2O and some volatiles like formaldehyde [22]. M-UF had a slow decomposition step, and $T_{5\%}$ was improved to 215□ because the bond energy of Si-O was bigger than C-O. UF decomposed rapidly but M-UF slowly during 250 to 350□, besides the residual masses of UF and M-UF were 24.0% and 70.3% respectively at 350□. Furthermore, the mass of char residue of UF was 11.4% but M-UF was 43.8% at 800□, which indicated that the amount of charring of M-UF was higher than UF. In addition, the $T_{5\%}$ of UF+KH-550 cal. was 72□ and the residual mass was 24.6% at 800□. Compared with UF+KH-550 cal., M-UF had higher decomposition temperature and residual mass significantly. The Fig.3b explained that the decomposition rate peak of UF and UF+KH-550 cal. appeared at 297□ and 300□ respectively, but the decomposition rate peak of M-UF was at 277□. Besides, the maximum decomposition rate of UF and UF+KH-550 cal. was bigger than M-UF. After reaching the peak, the decomposition rate of M-UF reduced to around 1 %/min at 400□ and kept invariant, and then the decomposition rate of M-UF was obviously lower than UF and UF+KH-550 cal.. The TGA and DTG stated that M-UF had higher thermal stability and charring-forming amount than UF and UF+KH-550 cal..

3.2 Flammability

The results of LOI and UL-94 vertically burning for PP composites are presented in Table 1. Table 1 showed that the LOI value of pure PP was 17 and it could not pass the UL-94 tests with a lot of molten drips. The LOI of PP-2 was 19.4, which illustrated APP had a little flame retardancy to PP, but PP-2 could not pass the UL-94 tests neither.

From PP-3 to PP-7, the LOI value of PP-4 was 23.5 as maximum and PP-3 was 21.7 as minimum, which suggested that the addition of UF improved the LOI values of PP composites to some extent, because the nitrogen in UF together with phosphorus in APP had a good flame retardant effect on PP. The LOI value of PP-11 was 29.5 as maximum and PP-9 was 27.5 as minimum in PP-8 to PP-11. Table 1 also showed that the LOI values of PP composites adding M-UF were higher than those adding the same amount of UF, because the nitrogen and silicon in M-UF cooperating with phosphorus in APP had a better flame retardant effect on PP. Besides, PP-8 to PP-11 all could pass UL-94 tests and reach V-0. Hence, the results of LOI and UL-94 tests explained that M-UF/APP had a better flame retardant effect on PP compared with the same loading of UF/APP.

Some of the flame-retardant PP composites were studied by micro combustion calorimetry (MCC), all of them were repeated three times and the deviation of these data was within ±10%. Table 3 shows the heat release capacity (HRC), thermal release rate peak (PHRR) and corresponding temperature (T_{PHRR}) and total heat release (THR) [23]. PHRR in MCC is regarded as one of the most important parameter to evaluate relevant flammability using mg specimen. The PHRR of PP-1 and PP-2 were 1028.4W/g and 738.8W/g respectively, and the PHRR of PP-2 was reduced about 28% compared with PP-1. In addition, the PHRR of PP-6 and PP-11 were further reduced into 722.1W/g and 645.4W/g respectively, which correspondingly decreased 30% and 37% compared with PP-1. It indicated that the susceptibility of PP-11 to fire was lowest among these four PP composites in MCC. The HRC is defined as the PHRR divided by the nominal heating rate (1°C/s). The HRC of PP-11 was lowest that represented a best flame retardance in these four PP

composites [24]. Thermal release rate curves of PP composites are presented in Fig.4. The T_{PHRR} of these four PP composites were in 487 ± 5□, which explained that the main thermal decomposition progresses were no great difference [25]. To sum up, PP-11 shows a lowest susceptibility to fire and best flame retardancy, but its flame retardant performance is not remarkable here.

Table 3 MCC tests results of some PP composites.

Samples	HRC ($J \cdot g^{-1} \cdot K^{-1}$)	PHRR (W/g)	T_{PHRR} (□)	THR (kJ/g)
PP-1	**1038.5**	**1028.4**	**482**	**40.2**
PP-2	**769.6**	**738.8**	**492**	**28.6**
PP-6	**723.5**	**722.1**	**489**	**25.7**
PP-11	**652.0**	**645.4**	**490**	**21.3**

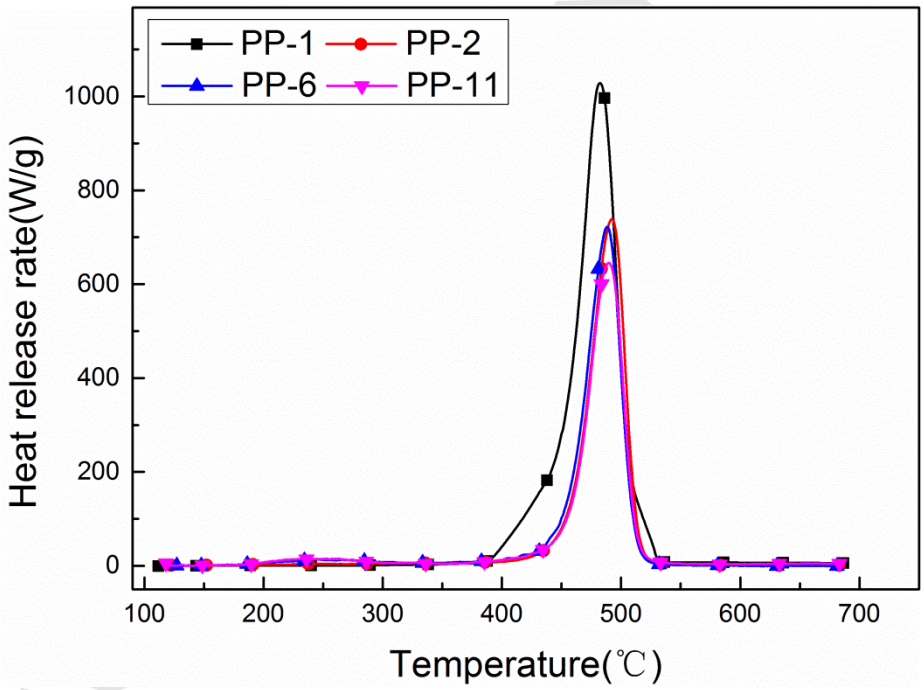

Fig.4 HRR of some PP composites obtained from MCC.

3.3 Thermal analysis

Thermogravimetric analysis results of some PP composites are presented by Fig.5a (TG), Fig.5b (DTG) and Table 4. PP-1 had only one decomposition step beginning at 410□ and the residual mass was 0 at 800□, which illustrated that pure PP could not form char itself. PP-2 had an obvious decomposition step beginning at 380□. The

phosphoric acid and metaphosphoric acid released from APP might prompt PP to form fairly stable cross-linked residual char on the basis of dehydration mechanism of carbocation [26, 27]. Finally, the mass of residual char of PP-2 was 8.5% at 800□.

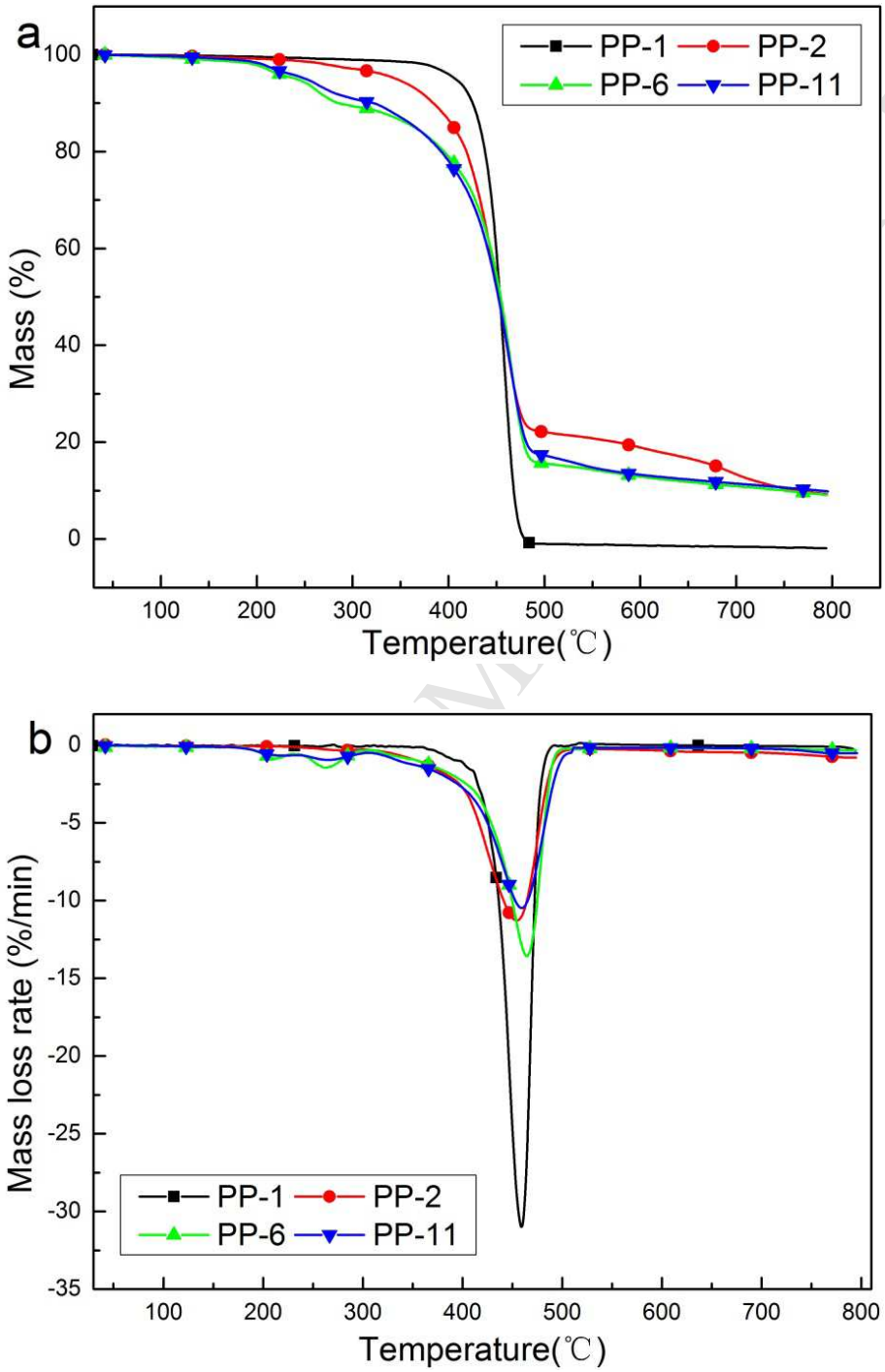

Fig.5 The TG (a) and DTG (b) curves of some PP composites

Table 4 TGA (a) and DTG (b) data from thermal decompositions of PP composites

Samples	Temperature (□)		CR (%)		R_{max} (%/min)
	$T_{5\%}$	T_{max}	350 □	800 □	
PP-1	**410**	**460**	**98.5**	**0**	**31.3**
PP-2	**380**	**477**	**96.2**	**8.5**	**16.6**
PP-6	**246**	**480**	**88.6**	**9.5**	**18.2**
PP-11	**260**	**475**	**90.4**	**10.4**	**15.8**

R_{max}: the maximum decomposition rate; CR: the char residue mass; T_{max}: the temperature of maximum decomposition rate.

PP-6 had three decomposition steps beginning at 246□. APP and UF in PP-6 might release small molecules like NH_3 in 200-250□ [28]. The polyphosphoric acid generated by APP might react with undecomposed UF to form slightly stable product 1 (p-1). During 250-350□, p-1 might further decompose to release ammonia, formaldehyde, phosphoric acid, metaphosphoric acid and so on. Those released acid might prompt PP to form cross-linked char. Finally, PP-6 mainly decomposed in the range of 400-550□ and the residual char mass was 9.5% at 800□. The $T_{5\%}$ of PP-11 was 260□ that was higher than PP-6. PP-11 had three decomposition steps as well and the mechanism of the first decomposition step was similar to PP-6. However, after releasing NH_3, APP might react with M-UF to form Si-O-P and Si-O-Si cross-linked product 2 (p-2) and product 3 (p-3). This might be the reason why the residual mass of PP-11 was higher than PP-6 at 350□. On the one hand, p-2 and p-3 might further cross-link to form char layer with temperature increasing. On the other hand, acids released from p-2, p-3 and APP might also prompt PP to from cross-linked char like PP-6. Finally, the residual char mass of PP-11 was 10.4% at 800□. The $T_{5\%}$ of PP-6 and PP-11 were clearly lower than PP-1, because the initial decomposition temperatures of additives APP, UF and M-UF were obviously lower than pure PP. Therefore, the adding of UF/APP and M-UF/APP did not improve the initial decomposition temperatures and they were decomposed ahead of PP. The maximum decomposition rate of PP-11 was the lowest. However, T_{max} were ranged

from 460 to 480□ without significant difference for these four PP composites , which were in agreement with the T_{PHRR} in MCC.

There was no great difference in decomposition process between PP-6 and PP-11, but decomposition and char forming mechanisms might be different. The possible decomposition mechanisms of PP composites are shown in Scheme 2.

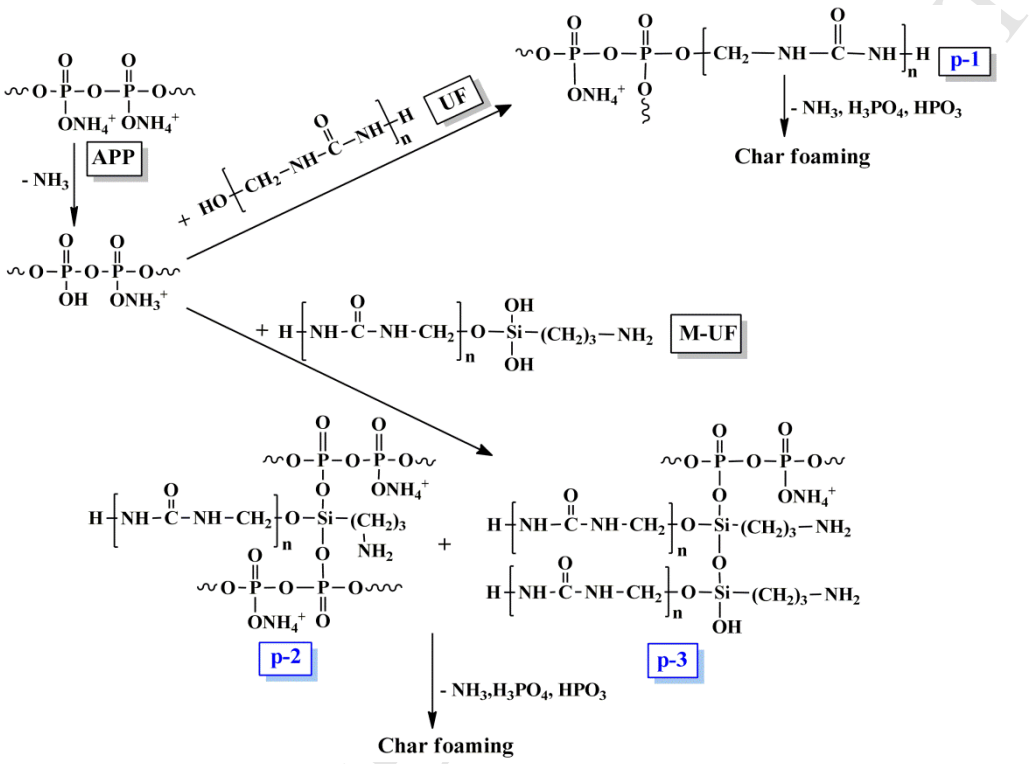

Scheme 2 The possible mechanisms of pyrolysis and char forming for IFRs (UF/APP and M-UF/APP) and PP composites.

It is significant to know the components of residual char for further explaining pyrolysis mechanisms. Therefore, PP-11 residual chars, obtained through Muffle furnace at 350, 600 and 800□, were tested by FT-IR and EDS. Fig.6 presents the results of FT-IR and EDS. The peaks of NH_4^+ at 3050-3320cm^{-1} decreased at 600□ and disappeared at 800□, explaining the further decomposition of NH_4^+. The peaks of $-CH_3$ at 2960 and 2870 cm^{-1} and $-CH_2-CH_2-$ at 2920 and 2830cm^{-1} still existed at 350□, which was consisted with the main decomposition in TGA. Besides, they decreased with the increasing of temperatures, which indicated the decomposition of main chain for PP-11. The peak at 1642cm^{-1} became wider, indicating the appearance of C=C. The peaks of 970, 1080, 1166 and 1255cm^{-1}, belonging to the symmetrical

stretching vibration of P-OH in HPO_4^{2-} and $H_2PO_4^-$, PO_3 in HPO_4^{2-}, PO_2 in $H_2PO_4^-$ and PO_2 in PO_3^-, decreased at 600□ and disappeared at 800□ [27]. It suggested that APP was gradually decomposed with temperature increasing. Furthermore, the peak at 1020cm^{-1} might belong to P-O-Si and Si-O-Si appeared at 350□ and became wider at 600 and 800□, indicating the producing of cross-linked structure p-2 and p-3. The EDS data investigated the contents of carbon (C), nitrogen (N), oxygen (O), and phosphorus (P). The content of C was reduced at 600□ due to the oxidation of unstable C, and increased a little for the information of stable C=C [28]. The content of N was kept decreasing because of the release of NH_3. Besides, the content of O had increased at 600□ because the release of H_2O was reduced, and further decreased at 800□ for the further release of H_2O and H_3PO_4, etc. However, the contents of Si and P were increased. It might be because of the formation of stable cross-linked structure P-O-Si and Si-O-Si and the decreases of other elements.

Elements	C (wt%)	N (wt%)	O (wt%)	Si (wt%)	P (wt%)
350 ℃	73.5	4.7	17.8	0.3	3.7
600 ℃	38.9	3.6	43	0.7	13.8
800 ℃	42.5	2.8	21	3	30.7

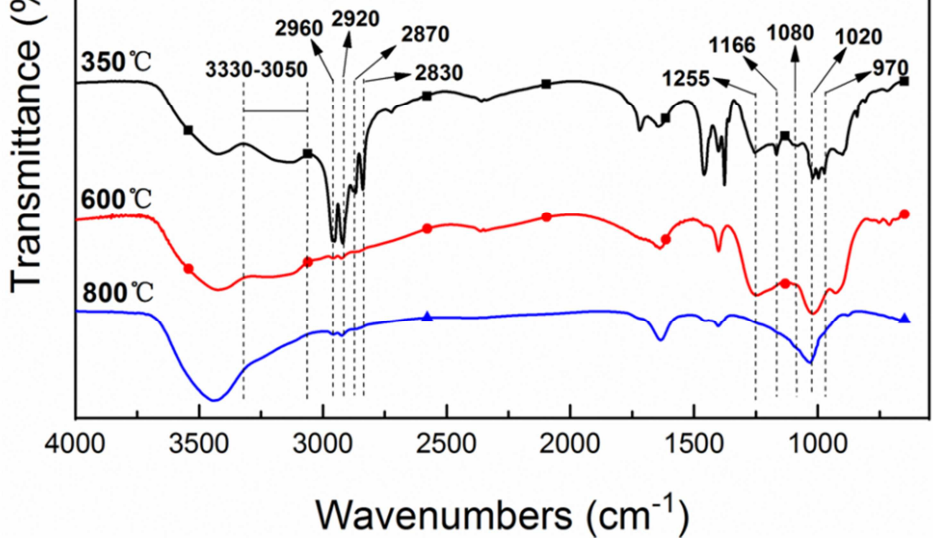

Fig.6 The results of FT-IR and EDS for PP-11 residual char at different temperatures.

3.4 Analysis of residual char

The strength of char layer has a great connection with its degree of graphitization. The degree of graphitization is higher; the strength of residual char is bigger [4, 29]. Fig.7 shows the Raman spectra of residual char after LOI testing for PP-6 and PP-11. The peaks of 1591cm^{-1} and 1366cm^{-1} were respectively belonging to the vibration of SP^2 G-band for integrally graphited carbon and SP^3 D-band for amorphous carbon. Generally, the ratio of peak area was used to explain the degree of graphitization. The analytic results of graphitization were illustrated in Table 5, which were obtained through Gauss method for peak-fit processing and peak area calculating. A_D and A_G were peak areas of D-band and G-band respectively, and R was the ratio of A_G to A_D. The R of PP-11 was bigger than PP-6, which illustrated the degree of graphitization and the strength of PP-11 char layer was greater than PP-6.

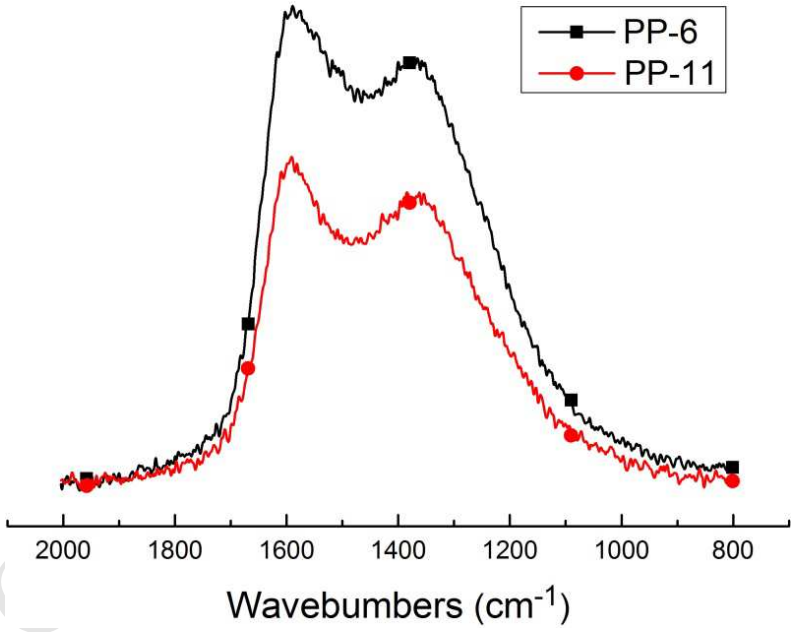

Fig.7 The residual char's Raman spectra for PP-6 and PP-11.

Table 5 The analytic results of graphitization obtained from Roman spectra

Samples	A_D	A_G	R
PP-6	**40885**	**49924**	**1.22**
PP-11	**38406**	**60204**	**1.57**

The compactness of residual char has a significant influence on the flame retardant effect. The strong ability of isolating heat and oxygen depends on compact residual char [30]. The actually combusting conditions after LOI tests and FE-SEM of corresponding residual chars are presented in Fig.8. As shown by Fig.8a, PP-2 had melting drips without obvious char layer and its surface was smooth. PP-6 had a little residual char and its surface had obviously inconsecutive and large hole, which were illustrated by Fig.8b. Fig.8c showed that PP-11 evidently had intumescent char layer, and the surface of residual char layer was consecutive and compact with little hole.

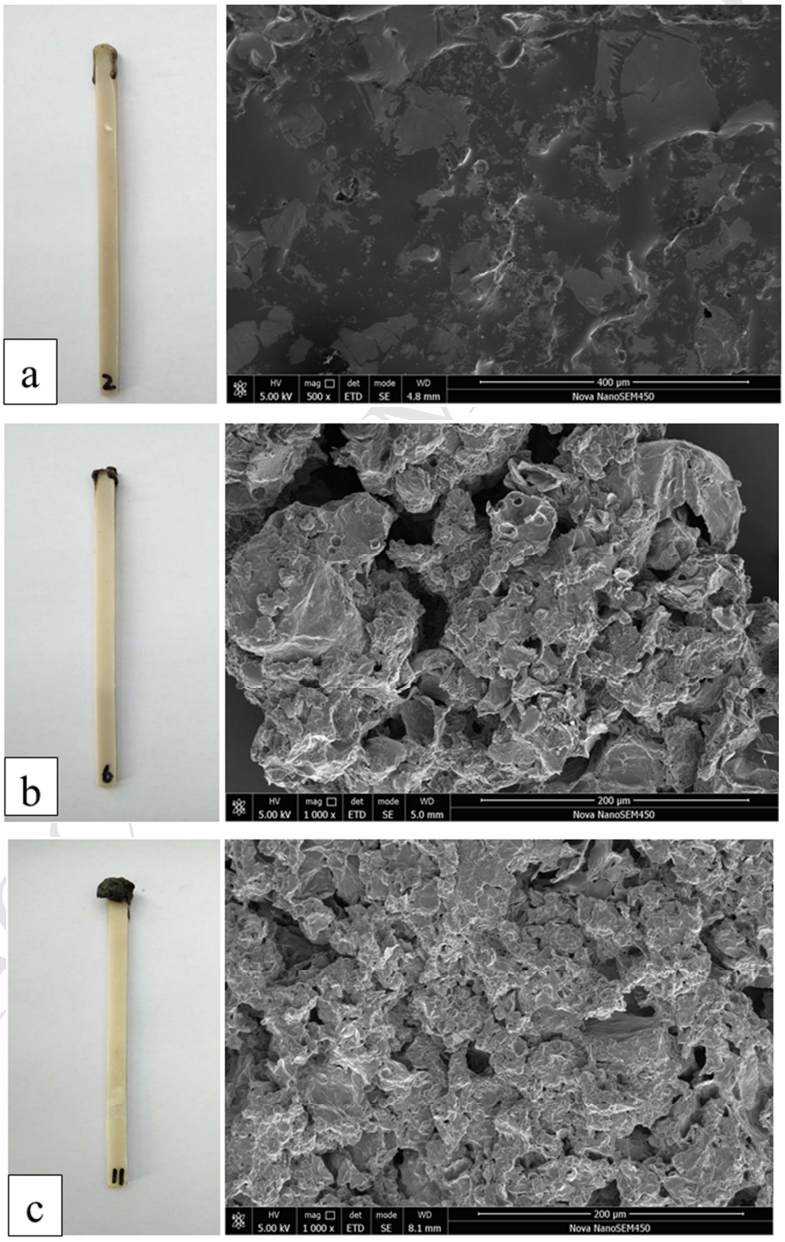

Fig.8 The actual combustion result photographs and SEM of residual char for PP-2 (a), PP-6 (b) and PP-11 (c).

For PP-6, phosphoric acids generated by p-1 and APP might cause PP to dehydrate forming low-intensive char layer so that the released inert gases like NH_3 might break through it, which results in loose and multi-hole char layer. Thus such char layer might not only further burn but also generate molten drips. For PP-11, the high-intensive cross-linked char layer formed by p-2 and p-3, together with low-intensive char layer formed by PP through phosphoric acids catalyzing, might resist inert gases so that they are compact and consecutive. These char layers might cover on PP and prevent further combustion. Therefore, M-UF+APP/PP might form more effective char layer compared with UF+APP/PP, and the former had better flame retardant efficiency.

3.5 Tensile properties of some PP composites

The results of tensile tests are presented by Fig.9 and Table 6. The break strength of PP-1 was 26.3MPa with 17.8% breaking elongation, which showed “cold drawing” behavior. Pure PP was crystallographic polymer and expressed crystalline and high-elastic state at room temperature. The break strength of PP-2 reduced to 20.30MPa and the breaking elongation and breaking energy were lower than PP-1, because the addition of APP damaged the crystal structure of PP. The break strength of PP-6 was 17.9MPa that was lower than PP-2. The breaking elongation and breaking energy of PP-6 were also lower than PP-2, which illustrated that the addition of UF further damaged the crystal structure of PP. In addition, the break strength of PP-11 was bigger than PP-6, but it was lower than PP-2. Besides, the breaking elongation and breaking energy of PP-11 were larger than both PP-2 and PP-6. On the one hand, the addition of M-UF as similar as UF could damage the crystal structure of PP. On the other hand, the flexible Si-O in M-UF improved the toughness of PP composites. In terms of break strength, PP-11 may be used in automotive parts such as handle and saucer [31, 32].

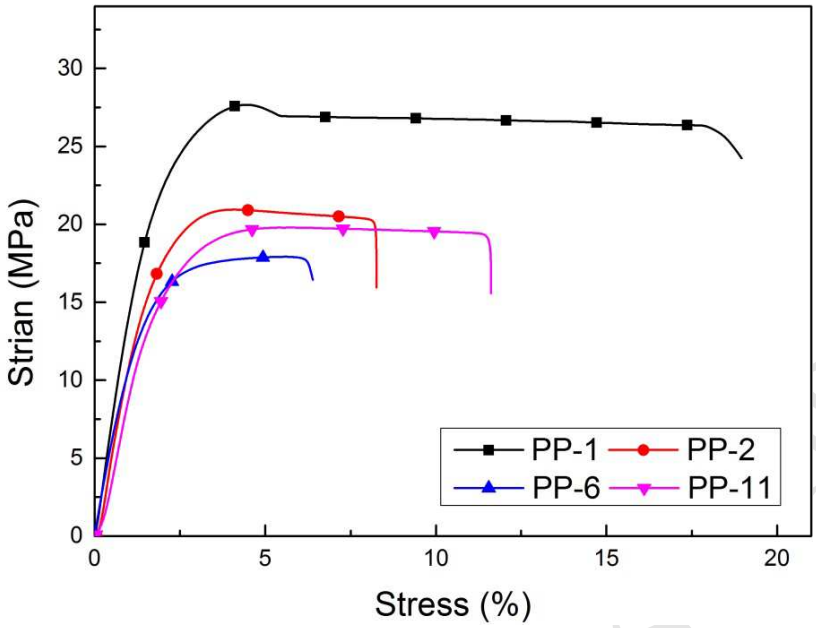

Fig.9 The strain-stress curves of some PP composites.

Table 6 Tensile testing results of some PP composites.

Samples	PP-1	PP-2	PP-6	PP-11
Break strength (MPa)	**26.3**	**20.3**	**17.9**	**19.4**
Breaking elongation (%)	**17.8**	**8.2**	**5.6**	**11.4**
Breaking energy ($J \cdot m^{-3}$)	**476.2**	**147.6**	**96.3**	**201.6**

4. Conclusions

KH-550 successfully modified UF and introduced into flame retardant element silicon. Compared with UF, M-UF had higher thermal stability and residual char mass. Compared with PP/APP/UF, PP/APP/M-UF had better flame retardant effects in terms of LOI values and UL-94 testing grades, which was attributed to the higher mass and strength of char layer. TGA results and residual char analyses explained the decomposition and flame retardancy mechanisms of PP composites. Furthermore, they showed the reasons why the flame retardant efficiency of PP/APP/M-UF was better than PP/APP/UF. Tensile tests illustrated that PP-11 still might be applied in practice.

5. Acknowledgments

We thank the strongly supports by the following: the Experiment Center of Polymer Science and Engineering Academy, Sichuan University

6. References

References:

1. Green, J., The Flame Retardation of Polyolefins Flame-Retardant Polymeric Materials, 1982: p. 1-2.
2. Lim, K.-S., et al., A review of application of ammonium polyphosphate as intumescent flame retardant in thermoplastic composites. Composites Part B: Engineering, 2016. **84**: p. 155-174.
3. Li, B. and M. Xu, Effect of a novel charring–foaming agent on flame retardancy and thermal degradation of intumescent flame retardant polypropylene. Polymer Degradation and Stability, 2006. **91**(6): p. 1380-1386.
4. Feng, C., et al., Synergistic effect of La2O3 on the flame retardant properties and the degradation mechanism of a novel PP/IFR system. Polymer Degradation and Stability, 2012. **97**(5): p. 707-714.
5. Yan, S., Reserch Progress of PP Flame Retardant Systerm. Morden Plasticis Processing and Applications, 2007. **19**(6): p. 61-64.
6. Wen, P., et al., One-pot synthesis of a novel s-triazine-based hyperbranched charring foaming agent and its enhancement on flame retardancy and water resistance of polypropylene. Polymer Degradation and Stability, 2014. **110**: p. 165-174.
7. Johns, W.E. and A.K. Dunker, Urea-Formaldehyde Resins. American Chemical Society, 1986. **316**: p. 76-86.
8. Conner, A.H., Urea-Formadehyde Adhensive Resins. Polymeric Materials Encyclopedia, 1996. **11**: p. 8596-8607.
9. Pratt, T.J., et al., A Novel Concept on the Structure of Cured Urea-Formaldehyde Resin. The Journal of Adhesion, 2007. **17**(4): p. 275-295.
10. Hamdani, S., et al., Flame retardancy of silicone-based materials. Polymer Degradation and Stability, 2009. **94**(4): p. 465-495.
11. Ni, J., et al., Preparation of gel-silica/ammonium polyphosphate core-shell flame retardant and properties of polyurethane composites. Polymers for Advanced Technologies, 2011. **22**(12): p. 1824-1831.
12. Wen, P., et al., Synthesis of a novel triazine-based polymeric flame retardant and its application in polypropylene. Polymer Degradation and Stability, 2016. **134**: p. 202-210.
13. Li, R. and J. Gu, The synthetic technology urea-formaldehyde resin with weak acidity initial condition. China Adehesives, 2006. **15**(4): p. 36-40.
14. Du, G., The influence of condensations conditions on the structure of UF resin. Adhesion, 2000. **21**(1): p. 13-16.
15. Zhao, J., J. Gu, and R. Ni, Study on the Synthetic Technology of Urea-formaldehyde Resin under Weak Acidity Condition. Chemistry and Adhesion, 2006. **28**(6): p. 389-393.
16. Liu, J. and G. Yao, Research on Hydrolysis Process of Silane Coupling Agent. China Powder Science and Technology, 2014. **20**(4): p. 60-63.
17. Gao, Z., X. Jiang, and K. Guo, Study of the hydrolysis of 3-aminopropyltriethoxysilane (KH-550) and the surface modification of silica. Journal of Beijing of Chemical Technology (Natural Science), 2012. **39**(2): p. 7-11.
18. Torry, S.A., et al., Kinetic analysis of organosilane hydrolysis and condensation. International

Journal of Adhesion and Adhesives, 2006. **26**(1-2): p. 40-49.

19. T.Zorba, et al., Urea-formadehyde resins characterized by thermal analysis and FTIR method. Journal of Thermal Analysis and Calorimetry, 2008. **92**(1): p. 29-33.
20. Ma, Z., J. Wang, and X. Zhang, Effect of silane KH-550 to polypropylene/brucite composite. Journal of Applied Polymer Science, 2008. **107**(2): p. 1000-1005.
21. Luo, Y., L. Gu, and L. Zhu, FTIR analysis of SyntheZing of Urea-formaldehyde Resin. Journal of Adhesion Sichuan Forestry Science and Technology, 2007. **28**(2): p. 77-80.
22. Kim, J., et al., Formaldehyde emissions from particle board made with phenol–urea–formaldehyde resin prepared by different synthesis methods. Journal of Adhesion Science and Technology, 2015. **29**(19): p. 2090-2103.
23. Xu, J., et al., Determination of Flammability of textiles by micro combustion calorimeter. Dyeing and Finishing, 2013. **18**: p. 38-39.
24. Chatterjee, S., K. Shanmuganathan, and G. Kumaraswamy, Fire-Retardant, Self-Extinguishing Inorganic/Polymer Composite Memory Foams. ACS Appl Mater Interfaces, 2017.
25. HAN Yi, L.G.p., Liu Yuan,Wang Qi Investigation on Magnesium Hydroxide Grafted with DOPO in Flame Retarding PP. CHINA PLASTICS INDUSTRY, 2013. **41**: p. 30-32.
26. Ge, S., Plastic Flame Retardant Practical Technology. Materials Flame Retardant Practical Technology, ed. S. Ding. 2004, Bei Jing: Chemical Industry Press.
27. Lin, H., et al., The influence of KH-550 on properties of ammonium polyphosphate and polypropylene flame retardant composites. Polymer Degradation and Stability, 2011. **96**(7): p. 1382-1388.
28. Shao, Z.-B., et al., Flame retardation of polypropylene via a novel intumescent flame retardant: Ethylenediamine-modified ammonium polyphosphate. Polymer Degradation and Stability, 2014. **106**: p. 88-96.
29. Qian, L., et al., Research on Polypropylene Composites Flame -retarded and Reinforced by APP/MCA. China Plastics, 2010. **24**(5): p. 81-84.
30. Xu, Z.-Z., et al., Flame retardant mechanism of an efficient flame-retardant polymeric synergist with ammonium polyphosphate for polypropylene. Polymer Degradation and Stability, 2013. **98**(10): p. 2011-2020.
31. Liu, B., China petrochemical commodity brochure. 2000: China Petrochemical Press.
32. Yong Tian, J.W., The Property and Application of Polypropylene Reinforce Material on Automotive. China Academic Journal Electronic Publishing House, 2012. **06**: p. 66-70.

The highlights: Firstly, considering UF high contents of carbon and nitrogen and cheap raw materials, UF and KH-550 modified UF (M-UF) as charring agents were studied by FE-SEM, EDS, FTIR and TGA. Secondly, the flame retardant efficiency were researched by LOI, UL-94 and MCC for UF+APP/PP and M-UF+APP/PP. Besides, the pyrolytic mechanisms were explained by TGA, FT-IR and EDS. The residual char analyzed by LRS and FE-SEM. The results indicated that M-UF+APP/PP had better flame retardant effects in terms of LOI values, UL-94 testing grades, and THR and PHRR values compared with UF+APP/PP. Tensile properties were studied as well, and the results illustrated that PP-11 might be applied in practice.